agronomy

MDPI

Article

Distribution Characteristics and Pollution Assessment of Soil Aggregates of Cr, Ni, and Cu in a Region of Northern Hebei Province

Sha Xie [1,2], Jie Zhang [1,2], Zhijun Liu [1,2], Xiaofei Guo [1,2], Yuebing Sun [3,4] and Qingqing Huang [3,4,*]

1 Hebei Huakan Resource Environmental Survey Co., Ltd., Chengde 067000, China; xiesha1995@126.com (S.X.); zhangminzai5516@163.com (J.Z.); lzj2014514@163.com (Z.L.); guoxiaofei7193@126.com (X.G.)
2 Hebei Provincial Key Laboratory of Geological Resources Exploration, Development and Ecological Protection, Chengde 067000, China
3 Key Laboratory of Original Agro-Environmental Pollution Prevention and Control, Ministry of Agriculture and Rural Affairs (MARA), Agro-Environmental Protection Institute, MARA, Tianjin 300191, China; sunyuebing@caas.cn
4 Tianjin Key Laboratory of Agro-Environment and Agro-Product Safety, Agro-Environmental Protection Institute, MARA, Tianjin 300191, China
* Correspondence: huangqingqing@caas.cn; Tel.: +86-17602209636

Abstract: In order to understand the distribution, occurrence forms, and influencing factors of chromium (Cr), nickel (Ni), and copper (Cu) in soil aggregates, a five-step extraction method was used to determine their forms in soil aggregates of different sizes in a mountainous area of northern Hebei Province. The ecological risk was evaluated using the geo-accumulation index (I_{geo}) and primary and secondary comparison value method (RSP). Redundancy analysis (RDA) was used to identify the main factors affecting the distribution and morphology of Cr, Ni, and Cu in soil. The results showed that in vertical distribution, Cr, Ni, and Cu were concentrated in the surface soil, but there was no clear relationship between soil depth and heavy metal content. The distribution characteristics revealed that Cr, Ni, and Cu in soils mainly existed in relatively stable Fe-Mn oxides and residue states, and their morphology in aggregates did not vary considerably with particle size. Furthermore, the RSP results showed that the pollution risk of Cr, Ni, and Cu was higher, with Cr and Ni posing the highest risk in the 0.5–1 mm and 1–2 mm particle size ranges. The RDA results showed that available phosphorus and soil organic matter (SOM) were the main factors that caused the characteristic difference of 1–2 mm aggregate components. Additionally, hydrolyzed nitrogen, cation exchange capacity (CEC), and calcium exchange have positive effects on the residual state of Cr. For Ni, SOM, CEC and exchangeable calcium have positive effects on the binding state of Fe and Mn oxides and carbonate. For Cu, CEC and exchangeable calcium are the key factors that cause the morphological differences of aggregates. Based on the above results, a theoretical basis has been provided for the prevention and control of pollution in the subsequent research area.

Keywords: distribution characteristics; risk assessment; aggregate; chromium; nickel; copper

check for updates

Citation: Xie, S.; Zhang, J.; Liu, Z.; Guo, X.; Sun, Y.; Huang, Q. Distribution Characteristics and Pollution Assessment of Soil Aggregates of Cr, Ni, and Cu in a Region of Northern Hebei Province. *Agronomy* **2024**, *14*, 2408. https://doi.org/10.3390/agronomy14102408

Academic Editor: Wanting Ling

Received: 13 September 2024
Revised: 13 October 2024
Accepted: 15 October 2024
Published: 17 October 2024

Copyright: © 2024 by the authors. Licensee MDPI, Basel, Switzerland. This article is an open access article distributed under the terms and conditions of the Creative Commons Attribution (CC BY) license (https://creativecommons.org/licenses/by/4.0/).

1. Introduction

Due to rapid development in agriculture and industry, as well as inefficient waste treatment, heavy metal pollution in the environment has gotten attention. Heavy metals, as a category of highly hazardous pollutants, are particularly concerning due to their toxicity, non-biodegradability, and potential for bioaccumulation in food chains, resulting in biomagnification and heightened health risks for people [1,2]. Even some trace heavy metal elements, such as chromium (Cr), nickel (Ni), and copper (Cu), which are essential for maintaining life, can cause irreversible damage to organisms if the limit is exceeded [3,4]. Heavy metals in the environment enter the human body mainly through the food chain,

with the primary route of entry being the consumption of polluted staple crops [5]. Furthermore, heavy metal pollution is detrimental to soil ecosystems, negatively impacting both biotic and abiotic components.

The problem of soil pollution worldwide is very serious. Some researchers assessed the mercury pollution in Ratai Basin caused by artisanal and small-scale gold mining activities in Nampong Province, Indonesia and found that the soil mercury pollution caused by erosion was very serious [6]. In Spain, some scholars have discussed the influence of mineral transportation in historical mining areas on soil pollution along the old railway and found that the topsoil along the railway is extremely acidic in the reaction. Compared to the local background concentrations, high concentrations of lead, zinc, copper, arsenic, mercury, and antimony have been detected in the railway line, indicating that there is serious human pollution [7]. Some scholars also evaluated the heavy metal pollution in the soil around the oil refinery in Salahuddin province, Iraq. The results show that all sites are highly polluted by chromium, nickel and molybdenum [8]. Therefore, soil pollution and ecological risks associated with heavy metals deserve special attention.

Soil aggregates are the fundamental constituent units of soil structure, therefore, understanding the distribution, forms, and characteristics of heavy metals in soil aggregates is critical for determining heavy metals contamination behavior [9]. Currently, the majority of research focuses on the morphological and geographical distribution of heavy metals, particularly the speciation distribution characteristics and hazard risk assessment of heavy metals in aggregates. Actually, rather than in the soil, a significant portion of the chemical reaction take place within the aggregate. The behavior of heavy metals in soil is largely constrained by aggregates distribution, thereby affecting their bioavailability and migration ability [10].

Currently, researchers both domestically and internationally are engaged on a number of studies to investigate the morphological risks and spatial distribution properties of heavy metals in soils and aggregates of different particle sizes. Fuling Zhang et al. [11] used a series of statistical methods to analyze the spatial distribution and ecological risk of heavy metals in soil, and found that Zn, Cu, Pb, and Cd in grassland soil around the mining area were mainly affected by human activities, whereas Cr and Ni were mainly affected by soil geochemistry. Qiang et al. [12] found that the simultaneous enrichment of heavy metals in soil aggregates by various crops could produce antagonistic effects, and that the smaller the particle size of soil aggregates, the greater the total potential ecological risk. Deng et al. [10] obtained similar results that the majority of metal elements associated with soil aggregates showed a small drop in content as aggregate size increased, and changes in land use can have varying effects on the amounts of heavy metals linked to soil aggregates. Cui et al. [13] used wet and dry screening tests to study the mechanism of heavy metal distribution and stability in soil aggregates of different particle sizes. The results showed that the distribution of heavy metals with strong biological activity in wet soil aggregates is not controlled by aggregate stability but may be affected by soil organic carbon.

In this paper, the content distribution and occurrence forms of Cr, Ni, and Cu in horizontal, vertical, and aggregates with varying particle sizes were analyzed. The pollution level and ecological risk of Cr, Ni, and Cu were evaluated using the I_{geo} and the RSP method, respectively. The effects of physicochemical properties of aggregates of different particle sizes on the morphology of heavy metals were investigated by redundancy analysis, in order to provide scientific basis for further research on the migration and morphological transformation mechanism of Cr, Ni, and Cu in soil. This work can provide scientific basis for further study on the migration and transformation mechanism of soil Cr, Ni, and Cu and provide technical support for comprehensive control of soil Cr, Ni, and Cu pollution in the study area and surrounding farmland.

2. Materials and Methods

2.1. Study Area Profile

This project takes the farmland of a region in northern Hebei, China as the research area, which has a temperate continental monsoon climate. In the research region, the four seasons are distinct, and the climate is humid, with an average annual temperature of 8.6 °C. The mountainous landform area belongs to the generalized Yanshan Mountains, and the soil types are mainly brown soil and cinnamon soil. The total investigation area is about 351,029 m^2, and prior investigations of soil heavy metal contamination in this region have revealed the presence of Cr, Ni, and Cu pollutants. Therefore, the object of investigation in this paper is mainly concerned with Cr, Ni, and Cu. Eight inquiry units were created within the research region based on the landform, geography, and crop planting.

2.2. Sample Collection and Processing

A total of 54 surface soils (0–20 cm), 8 sectional samples were collected in the study area (Figure 1), among which 3 subsurface soils (20–50 cm) were collected at sites 1-1, 7-1, and 8-1 of the heavily polluted plots to investigate the content and spatial distribution characteristics of heavy metals in aggregates of different particle sizes in the study area (Figure 1). After being gathered, the soil samples weighing an average of 5 kg were transported to the lab in resealable plastic bags. Non-soil materials, such gravel and plant leftovers, were taken out, allowed to air dry, naturally ground in the lab, and then blended after screening to ascertain their fundamental chemical and physical characteristics. The aggregates having particle sizes of <0.25, 0.25–0.5, 0.5–1, and 1–2 mm, respectively, were screened using the wet screening method in order to determine the heavy metal content, morphological distribution characteristics, and risk assessment.

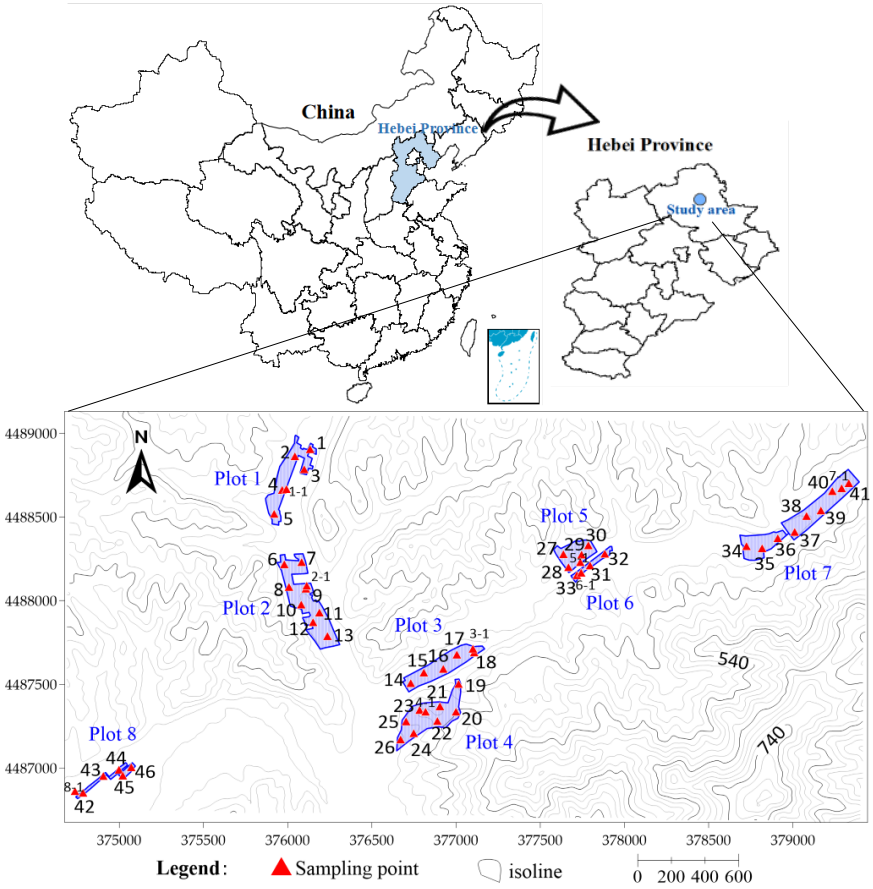

Figure 1. Layout of sampling points in the research area.

2.3. Methods of Soil Sample Analysis

The basic physical and chemical of the field soil were analyzed based on the methods of Lu [14]. The soil pH value was measured using a pH electrode (PB-10; Sartorius, Göttingen, Germany) at a ratio of soil to water of 1:2.5. The SOM was measured according to the Walkley–Black wet digestion method. The available nitrogen in the soil was determined using the alkaline hydrolysis method. Available phosphorus was determined using the ascorbic acid–ammonium molybdenum method. Available potassium was extracted with ammonium acetate and determined by flame photometry. The CEC was determined by ammonium acetate exchange method (pH = 7.0). The total concentration of Cr, Ni, and Cu in the soil (0.2500 g) was digested in an electrothermal digester (DigiBlock ED54, LabTech, Beijing, China) using 8 mL HNO_3 (guaranteed reagent) and 4 mL hydrofluoric acid (HF) (guaranteed reagent) at 120 °C for 1.0 h, and 150 °C for 2.0 h, respectively. The digestion process was complete when the digested solutions were 1–2 mL in volume. The digested solutions were then diluted to 50 mL with deionized water, filtered, and analyzed with ICP-MS (iCAP Q; Thermo Fisher Scientific, Waltham, MA, USA). Tessier five-step continuous extraction method was used to determine the morphological composition of heavy metals in soil samples, and the heavy metals were divided into exchangeable state (F1), carbonate bound state (F2), iron and manganese oxide bound state (F3), organic bound state (F4) and residue state (F5). The specific process is as follows: exchangeable fraction (F1; extracted with 1.0 M of $MgCl_2$, pH = 7), carbonate-bound fraction (F2; extracted by 1.0 M CH_3COONa, pH = 5), iron- and manganese-oxide-bound fraction (F3; extracted by 0.04 M $NH_2OH{\cdot}HCl$ in 25% CH_3COOH solution), organic-matter-bound fraction (F4; extracted by 0.02 M HNO_3 and 30% H_2O_2), and residual fraction (F5; digested with HNO_3-HF-$HClO_4$). The soil available Cr, Ni, and Cu was extracted using diethylenetriaminepentaacetic acid (DTPA) solution (0.005 M DTPA, 0.01 M $CaCl_2$, and 0.1 M triethanolamine, pH = 7.3) at a ratio of 1:5 (soil to DTPA solution). To guarantee the analytical accuracy of heavy metal content determination, all reagents employed during measurements are of superior purity. The standard soil reference material (SRM2586, National Institute of Standards and Technology, NIST, Gaithersburg, MD, USA) and blanks were included for quality control, and the recovery rates of soil sample were 80–120%. Three groups of duplicate samples are employed for all cases, with a maximum 15% variance of content between replicates.

2.4. Pollution Assessment Approach of Heavy Metals

2.4.1. The Geoaccumulation Index

The I_{geo} is typically used to assess the level of soil-based heavy metal pollution resulting from either natural or man-made sources [15,16]. The calculation formula is as follows:

$$I_{geo} = log_2 \frac{C_N}{K \times B_n} \quad (1)$$

where I_{geo} Represents the geoaccumulation index of heavy metals in soil samples; C_n is the measured value of heavy metal in soil samples, $mg{\cdot}kg^{-1}$; B_n is the geochemical background value of heavy metal, $mg{\cdot}kg^{-1}$. The relationship between the classification standard of soil accumulation index and pollution degree is shown in Table 1.

Table 1. Ecological risk assessment index grading standards.

I_{geo} Index	Pollution Assessment	RSP Index	Pollution Assessment
$I_{geo} < 0$	No pollution	RSP ≤ 1	No pollution
$0 < I_{geo} \leq 1$	Light pollution	$1 <$ RSP ≤ 2	Light pollution
$1 < I_{geo} \leq 2$	Relatively moderate pollution	$2 <$ RSP ≤ 3	Moderate pollution
$2 < I_{geo} \leq 3$	Moderate pollution	RSP > 3	Heavy pollution
$3 < I_{geo} \leq 4$	Relatively heavy pollution		
$4 < I_{geo} \leq 5$	Heavy pollution		
$I_{geo} > 5$	Extremely heavy pollution		

2.4.2. Pollution Assessment Based on the Form of Heavy Metals

RSP is an evaluation method to judge the degree of element pollution based on the speciation of heavy metals [17]. At present, the RSP is widely used to evaluate the bioavailability of heavy metals and the pollution degree of potential bioactive components. According to geochemical sources, soil heavy metals can be divided into primary and secondary phases, and residual heavy metals existing in primary mineral properties are called primary phases, which are not bioavailable. Other forms of heavy metals are called secondary phases and have bioavailability [18]. In this study, the residual heavy metal content determined by Tessier's five-step continuous extraction method is the primary phase content, and the other forms are the secondary phase content. The distribution ratio between primary and secondary phases can indicate the degree of pollution. The calculation formula is as follows:

$$\mathrm{RSP} = M_{sec} / M_{prim} \quad (2)$$

where RSP is the distribution ratio of secondary phase to primary phase of heavy metals; M_{sec} is the content of heavy metal secondary phase, mg·kg^{-1}; M_{prim} is the primary phase content of heavy metals, mg·kg^{-1}. According to the results of RSP, soil pollution levels are classified, as shown in Table 1.

2.5. Methods of Data Processing

Mapgis 67 and Sufer 23 were used to draw sampling plot and pollution distribution maps. The data of metal content of aggregate weight were processed and calculated by SPSS software V.26.0. Origin 2024 (Origin Lab, Northampton, MA, USA) was used to graph the data results; the data processing and preparation for Pearson correlation and RDA analysis are also carried out utilizing Origin 2024 (Origin Lab, Northampton, MA, USA) and SPSS software V.26.0.

3. Results and Discussion

3.1. Spatial Distribution Characteristics of Heavy Metals and Soil Properties

According to the detection results of heavy metal and physical/chemical properties of soil (Table 2), in this study area, the soil pH ranges from 4.45 to 7.93, with most areas being non-acidified and non-alkalized, and a few areas being slightly acidified. According to the classification standard of soil nutrient in Table 3 [19,20], SOM and rapidly available potassium is relatively deficient, while available phosphorus is at medium level. The content distributions of available phosphorus, exchangeable K^+, and exchangeable Mg^{2+} were found to be significantly different based on the coefficient of variation results, suggesting that their spatial distribution was highly uneven. Investigation on the distribution of heavy metals in the soil in the study area showed that the average contents of Cr, Cu, and Ni were 195.9, 46.64 and 70.26 mg·kg^{-1}, respectively, which far exceeded the background values of soil environment in Hebei Province (68.30, 21.80 and 30.80 mg·kg^{-1}) and the whole country (66.00, 25.00 and 27.00 mg·kg^{-1}) [21]. Mapgis and other tools were used to conduct spatial interpolation analysis on the data obtained from the first sampling; the results were shown in Figure 2.

In the horizontal direction, the content of Cr in the surface soil of the study area varies greatly, ranging from 59.00 to 298.0 mg·kg^{-1}, in which the high-value areas of soil Cr are mainly distributed in Plots 2, 3, 5, 6, and 7, with the content above 200.0 mg·kg^{-1}, while the low-background areas are mainly distributed in Plots 4 and 8, with the content below 130.0 mg·kg^{-1}. The content of Cu in the surface soil of the study area ranges from 17.30 to 86.50 mg·kg^{-1}, in which the high-value areas of soil copper are mainly distributed in the north of Plot 1, the middle of Plot 3, Plot 5, and Plot 8, with the content above 50.00 mg·kg^{-1}, while the low-value areas are mainly distributed in Plot 4, with the content level below 30.00 mg·kg^{-1}. The content of Ni in the surface soil of the study area also varies greatly, ranging from 23.00 to 139.0 mg·kg^{-1}. Among them, the high-value areas of

soil nickel are mainly distributed in the north of Plots 1, 2, 3, and Plot 8, and the content is mainly above 70.00 mg·kg^{-1}, while the low-value areas are mainly distributed in Plot 4, and the content level is below 50.00 mg·kg^{-1}.

Table 2. Descriptive statistics of physical and chemical properties of soil in the study area (sample number: 54).

Item	Average Data	STD	Minimum	Maximum	CV *
pH	6.25	0.79	4.45	7.93	0.13
SOM	15.80 g·kg^{-1}	5.97	5.84	35.97	0.37
AP *	22.75 mg·kg^{-1}	20.27	3.01	109.2	1.03
Ava-Fe *	45.66 mg·kg^{-1}	6.96	14.46	71.1	0.56
H-N *	84.35 mg·kg^{-1}	19.1	11.63	142.4	0.34
AK *	96.19 mg·kg^{-1}	22.8	40.87	197.9	0.34
CEC	47 cmol cmol·kg^{-1}	3.91	5.59	24.24	0.32
E-K *	0.16 cmol (K^+)·kg^{-1}	0.09	0.11	0.76	0.71
E-Na *	0.29 cmol (Na^+)·kg^{-1}	0.09	0.17	0.55	0.32
E-Ca *	7.62 cmol ($\frac{1}{2}$ Ca^{2+})·kg^{-1}	2.22	3.38	12.67	0.29
E-Mg *	2.87 cmol ($\frac{1}{2}$ Mg^{2+})·kg^{-1}	1.89	0.98	9.45	0.64

* AP—available phosphorus, Ava-Fe—available iron, H-N—hydrolyzed nitrogen, AK—rapidly available potassium, E-K—exchangeable K^+, E-Na—exchangeable Na^+, E-Ca—exchangeable Ca^{2+}, E-Mg—exchangeable Mg^{2+}; CV—coefficient of variation.

Table 3. The classification standard of major soil nutrients.

Soil Nutrient Grading	pH	SOM (g·kg^{-1})	AP (mg·kg^{-1})	AK (mg·kg^{-1})
deficient	≤5.00	≤20.00	≤15.00	≤100.00
moderate	5.00–7.00	20.00–35.00	15.00–35.00	100.00–200.00
abundant	>7.00	>35.00	>35.00	>200.00

In the vertical section direction of soil, as shown in Figure 3, three heavy metal elements in the soil profile is as follows: Cr, Ni, and Cu in the profile samples all exist in Plot 1, Plot 2, Plot 7, and Plot 8, and Cr also exists in Plot 3 and Plot 4; three kinds of heavy metals were found to exceed the standard in the profile samples, mainly in the surface soil of various plots, and some plots were found to exceed the standard in the surface and deep layers. In the soil profiles of different plots, Plots 4 and 6 are relatively clean, and there is no pollution of heavy metal. With the increase in soil depth, there is no simple increasing or decreasing relationship between heavy metal contents. This demonstrates that human factors may be the cause of the Cr, Ni, and Cu pollution in various soil plots within the study area rather than the high background value of the soil.

3.2. Distribution and Pollution Characteristics of Heavy Metals in Soil Aggregates

According to the results of the first sampling, aggregate analysis with four particle sizes (<0.25 mm, 0.25–0.5 mm, 0.5–1 mm, 1–2 mm) and five-step speciation analysis of Cr, Ni and Cu were carried out on the surface and subsurface soils of three typical polluted plots (Plot 1, Plot 7, and Plot 8) in the study area. As shown in Table 4, the findings showed that the soil in plots 1 and 8 has a predominance of particles smaller than 0.25 mm. The distribution of these particles is also quite different, with the soil particles being fine and irregular. In plot 7, the particle size radio of 1–2 mm is relatively large, but the difference of different particle sizes is small, and the soil particles are coarse and uniform.

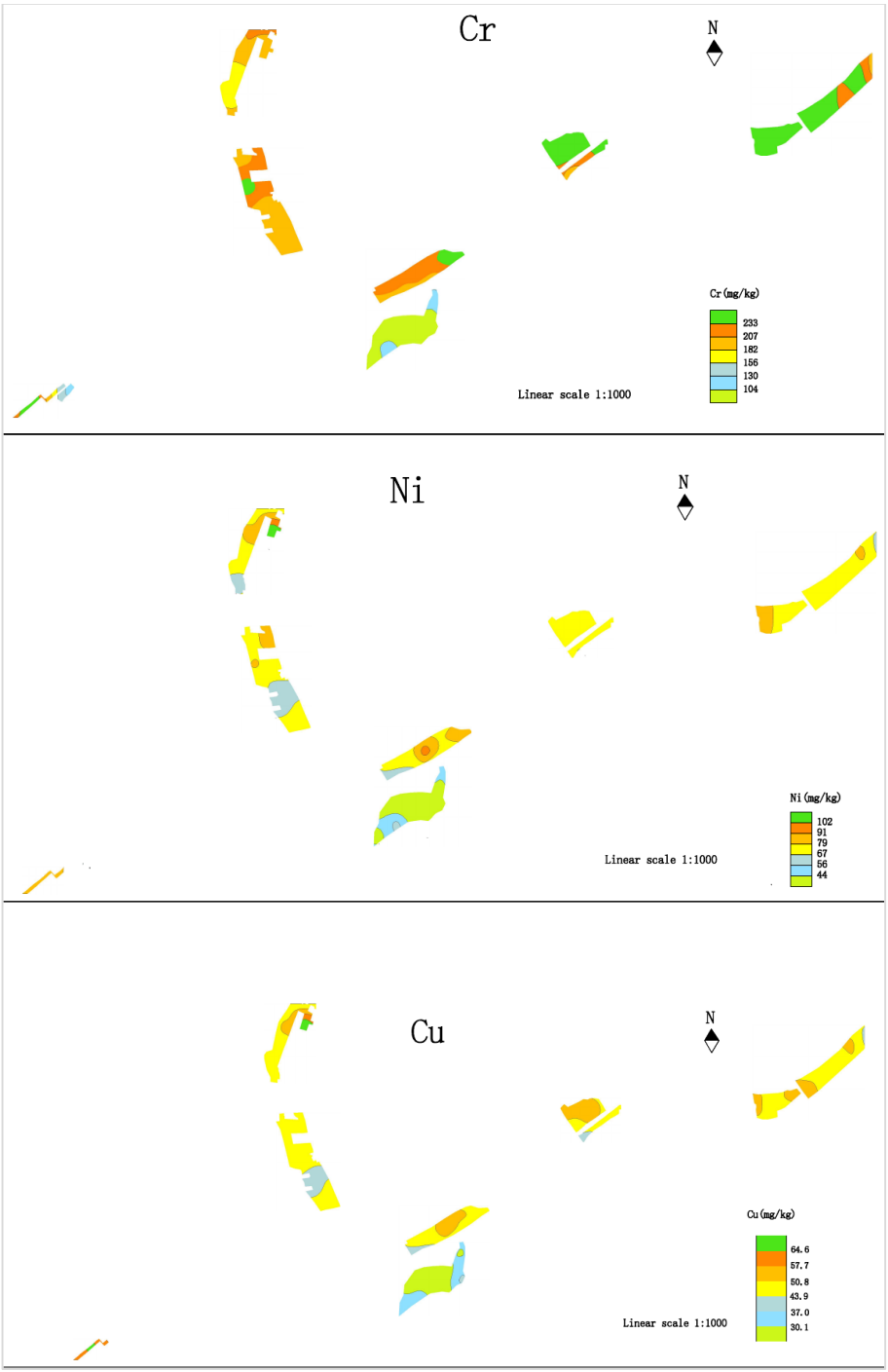

Figure 2. Spatial distribution of heavy metals Cr, Cu, and Ni in the study area.

Aggregates with varying particle sizes in various plots had varying heavy metal contents. The lowest content of three heavy metals in the majority of soil aggregates was found in particle sizes less than 0.25 mm, while the highest content was found in particle sizes between 0.25–0.5 mm. Following that, there was no discernible law of increase or decrease in the particle size range, but the heavy metal content slightly decreased. This tiny discrepancy in results could be attributed to the various size ranges of aggregates. According to some researchers, the heavy metal content rises as aggregate particle size decreases [22]. Large aggregates make up the majority of the size ranges in this study, with medium and micro aggregates primarily responsible for the latter [23].

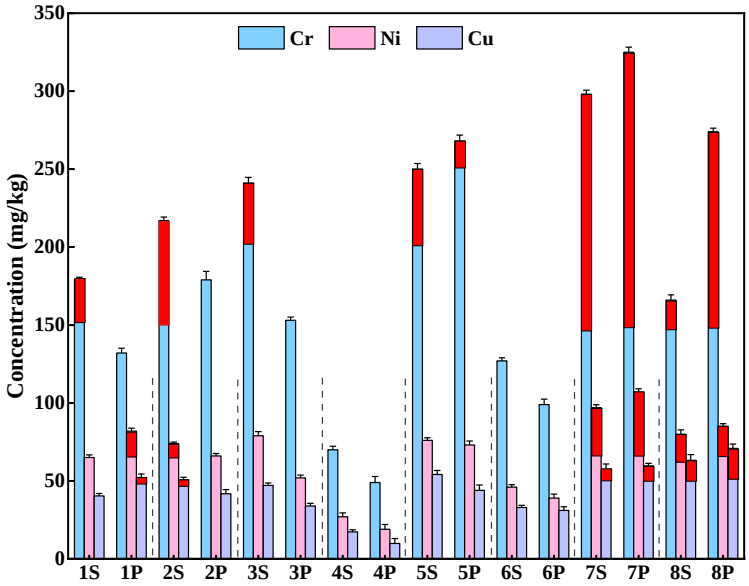

Figure 3. Distribution of Cr, Cu and Ni contents in different soil layers. Note: Numbers 1–8 represent different plots in the study area, "S" represents topsoil and "P" represents subsurface soil (20–50 cm), the red part represents that the value exceeds the threshold in the Soil environmental quality-Risk control standard for soil contamination of agricultural land (GB15618-2018).

Table 4. Analysis results of soil aggregates in different polluted areas (sample number: 18).

Sample	Particle Size (mm)	Weight (g)	Particle Size Load (%)	Cr ($mg \cdot kg^{-1}$)	Cu ($mg \cdot kg^{-1}$)	Ni ($mg \cdot kg^{-1}$)
P1-S *	<0.25 mm	59.62	61.5	64.64 ± 5.21	12.68 ± 1.87	38.86 ± 2.09
	0.25–0.5 mm	11.44	11.8	83.81 ± 6.40	17.03 ± 1.23	52.48 ± 4.31
	0.5–1 mm	14.21	14.66	68.43 ± 7.98	14.2 ± 1.05	43.83 ± 3.24
	1–2 mm	11.67	12.04	84.89 ± 7.01	16.63 ± 1.35	49.56 ± 4.36
P1-P *	<0.25 mm	71.33	72.81	65.52 ± 5.22	16.54 ± 1.77	40.85 ± 3.09
	0.25–0.5 mm	5.35	5.46	78.89 ± 6.89	19.03 ± 1.92	45.55 ± 3.77
	0.5–1 mm	13.42	13.7	67.12 ± 5.45	18.17 ± 1.80	46.31 ± 5.04
	1–2 mm	7.87	8.03	72.28 ± 6.97	15.6 ± 1.64	43.02 ± 4.57
P7-S *	<0.25 mm	25.27	25.58	120.4 ± 10.99	25.78 ± 2.09	63.58 ± 6.46
	0.25–0.5 mm	14.61	14.79	144.7 ± 11.24	28.36 ± 2.11	74.44 ± 7.79
	0.5–1 mm	9.82	9.94	139.3 ± 13.97	27.97 ± 2.36	66.92 ± 6.56
	1–2 mm	49.09	49.69	127 ± 13.15	27.03 ± 2.47	72.32 ± 6.88
P7-P *	<0.25 mm	27.37	27.82	101.9 ± 9.75	20.5 ± 1.98	54.93 ± 4.57
	0.25–0.5 mm	16.73	17.01	121.9 ± 10.78	22.57 ± 2.07	68.74 ± 5.62
	0.5–1 mm	26.11	26.54	118.2 ± 10.07	20.53 ± 1.96	56.22 ± 4.96
	1–2 mm	28.17	28.63	153.2 ± 13.29	22.4 ± 2.31	57.03 ± 4.79
P8-S *	<0.25 mm	48.15	48.94	113.3 ± 10.90	26.26 ± 2.38	48.07 ± 3.49
	0.25–0.5 mm	17.66	17.95	137.2 ± 11.04	32.44 ± 2.99	69.17 ± 4.98
	0.5–1 mm	19.76	20.08	115.6 ± 9.98	32.39 ± 2.02	57.39 ± 4.56
	1–2 mm	12.82	13.03	113.5 ± 9.79	34.3 ± 2.38	56.72 ± 5.69
P8-P *	<0.25 mm	38.8	39.61	97.42 ± 8.76	25.31 ± 2.34	48.2 ± 3.86
	0.25–0.5 mm	18	18.37	125.3 ± 11.09	37.32 ± 2.96	66.17 ± 6.08
	0.5–1 mm	22.92	23.4	108.1 ± 8.95	31.32 ± 2.09	55.25 ± 4.39
	1–2 mm	18.24	18.62	108.83 ± 9.03	34.84 ± 2.37	54.80 ± 4.01

* S represents the surface layer soil (0–20 cm), and P represents the subsurface layer soil (20–50 cm).

3.3. Distribution Characteristics of Heavy Metal Forms in Soil Aggregates

The speciation distribution of Cr, Ni, and Cu in different polluted areas is shown in Figure 4. Cr mainly exists in soil in residual state froms (F5), the proportion of this form in all particle size aggregates is above 50%, and the proportion of subsurface layer in polluted areas is similar to that of the surface layer. The bound states of iron and manganese oxide (F3) come next, making up roughly 10–30% of the total soil content. The amounts of Cr in

the exchangeable state (F1), carbonate-bound state (F2), and organic-bound state (F4) are all relatively tiny, falling within 10%, and the percentage of Cr in these three in surface soil is marginally higher than that of deep soil. The proportion of Cr in exchangeable state and carbonate bound state is extremely low, which indicates that the form of Cr in soil is stable and its bioavailability is low [24]. Among the aggregates with different particle sizes, the particle size ranges of 0.5–1 mm and 1–2 mm contain relatively little residual state, while the iron-manganese oxide bound states and carbonate bound states are relatively large.

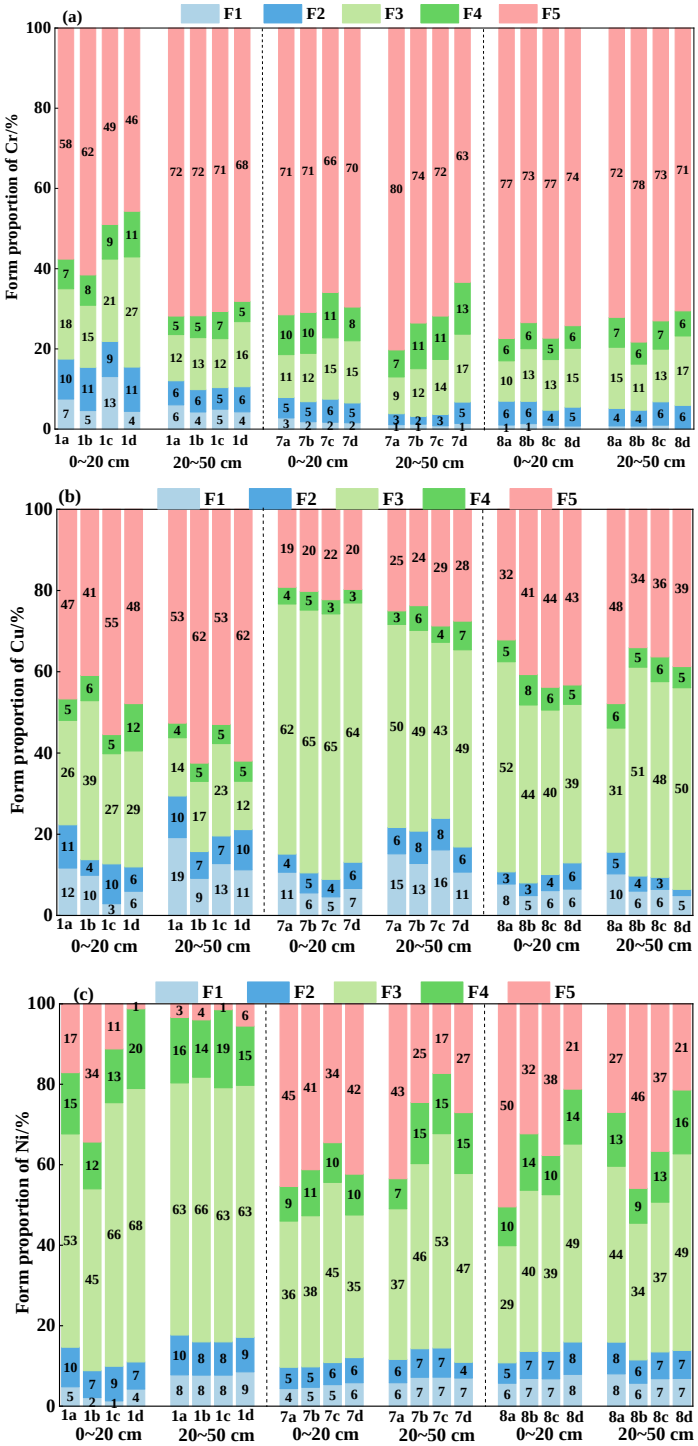

Figure 4. Speciation distribution of Cr (**a**), Cu (**b**), and Ni (**c**) in different polluted areas. Note: 1, 7, and 8 are the names of different plots; a, b, c, and d represent aggregates with particle size ranges of <0.25 mm, 0.25–0.5 mm, 0.5–1 mm, and 1–2 mm, respectively.

The main forms of Ni and Cu in soil are iron–manganese oxide bound states, followed by residual states, while Ni and Cu in exchangeable states, and carbonate-bound state account for a very low proportion, which indicate their forms are stable and their bioavailability is low [25]. This is consistent with the research results of Qin et al. [26]. Among them, the bound state of Fe-Mn oxide for Ni accounts for 29–68%, and the bound state of Fe-Mn oxide for Cu accounts for 12–65%. Soil pH in the study area is close to neutral, which is more conducive to the chelation (complexation) of iron and manganese oxides with soil heavy metals, resulting in the occurrence of heavy metals mainly in the binding state of iron and manganese oxides [27]. The variation of the forms for Ni and Cu with particle size in the aggregate is kind of different. For Ni, the proportion of Fe-Mn oxide bound state in aggregates with different particle sizes in Plot 1 is relatively high, while the residual state is relatively low. There is no significant difference in the proportion of exchangeable states and carbonate-bound states in the aggregates with different particle sizes. For Cu, the proportion of Fe-Mn oxide bound state in aggregates with different particle sizes in Plot 1 is relatively low, while the residual state accounts for a relatively high proportion. The exchangeable and carbonate-bound states with high bioavailability are relatively high in the small particle size range (<0.25 mm).

3.4. Pollution Assessment of Heavy Metal in Soil Aggregates

3.4.1. Geo-Accumulation Index Method

The I_{geo} of heavy metals in soil aggregates of different particle sizes in the study area is depicted in Figure 5. The I_{geo} value of Cr particle size ranges from 0.122 to 1.938, and the I_{geo} values of Cr in aggregates with particle sizes ranging from <0.25 mm, 0.25–0.5 mm, 0.5–1 mm, and 1–2 mm range from 0.255 to 1.938, 0.469 to 1.716, 0.226 to 1.500, and 0.126, respectively. The I_{geo} value of Cr in aggregates with different particle size ranges was mainly evaluated as relatively moderate pollution and light pollution, which did not reach the level of heavy pollution.

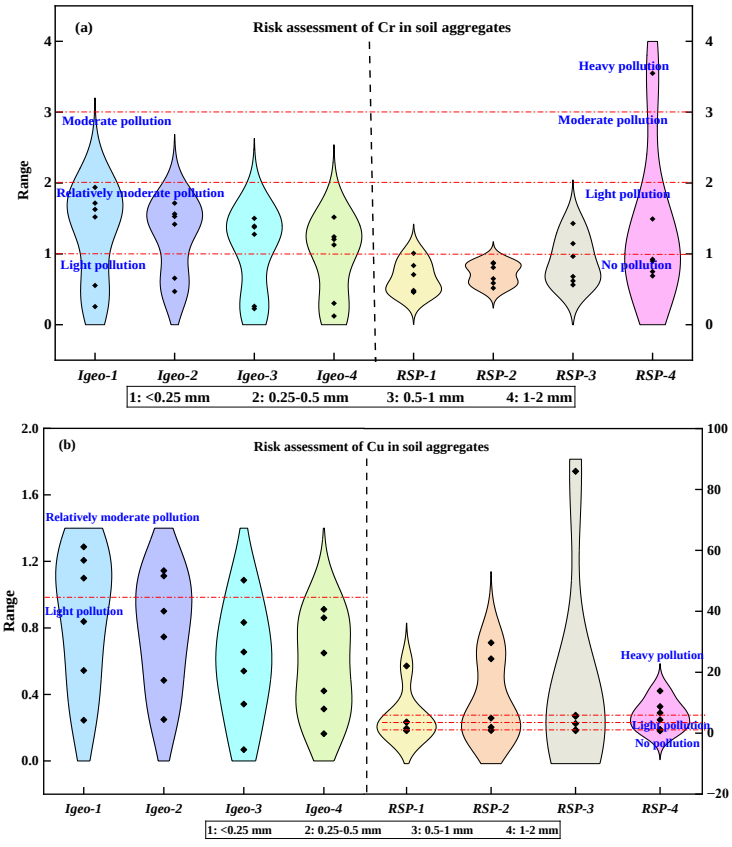

Figure 5. *Cont.*

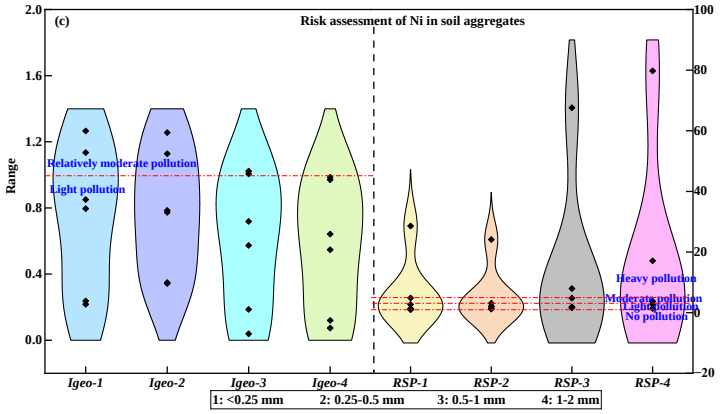

Figure 5. Evaluation results of Cr (**a**), Cu (**b**), and Ni (**c**) I_{geo} and RSP in soil aggregates of different particle sizes.

The I_{geo} value of Ni particle size ranges from 0.039 to 1.265, and the I_{geo} values of Ni in aggregates with particle sizes ranging from <0.25 mm, 0.25–0.5 mm, 0.5–1 mm, and 1–2 mm range from 0.217 to 1.265, 0.343 to 1.255, 0.039 to 1.023 and 0.075, respectively. The I_{geo} value of Ni in aggregates with different particle size ranges was mainly evaluated as relatively moderate pollution and light pollution, which did not reach the level of heavy pollution.

The I_{geo} value of Cu particle size ranges from 0.068 to 1.287. The I_{geo} values of Cu in the aggregates with particle sizes ranging from <0.25 mm, 0.25–0.5 mm, 0.5–1 mm and 1–2 mm are 0.245–1.287, 0.249~1.144, 0.068–1.087, and 0.164–0.912, respectively. Among them, the Cu pollution degree of 1–2 mm aggregates is only light pollution, and the other three particle sizes are mainly relatively moderate pollution and light pollution.

Among the three heavy metals under consideration, the relative order of I_{geo} is Ni < Cu < Cr, with Cr exhibiting the highest pollution degree. Overall, the I_{geo} values for Cr, Ni, and Cu generally decrease with increasing particle size; the highest pollution degree occurs in aggregates with a particle size < 0.25 mm, while lowest degree is observed in aggregates with a size of 1–2 mm. Only Cr and Ni aggregates within plot 1 exhibit the highest pollution degree at a particle size of 0.25–0.5 mm.

3.4.2. RSP Assessment Method

In addition to the damage of heavy metals in soil to the environment related to its total amount, the occurrence form of heavy metals also has a great stake in the impact of ecological environment [28].The RSP method was employed to assess the ecological risks posed by metals Cr, Ni, and Cu across varying particle sizes.

The results described in Figure 5 show that for particles with a particle size of 1–2 mm, Cr is heavily polluted at different points in the aggregate, while Cr is mainly pollution-free or slightly polluted in the aggregate with a particle size of 0.5–1 mm and mainly pollution-free in the particle size ranges of <0.25 mm and 0.25–0.5 mm. Ni shows heavy pollution in soil aggregates with different particle sizes, and the particle size range of 1–2 mm has the most serious pollution. Cu shows heavy pollution in aggregates with different particle sizes, and the particle size range of 0.5–1 mm has the most serious pollution. The results of heavy metal risk assessment based on RSP cumulative index show that Cr and Ni with particle sizes of 0.5–1 mm and 1–2 mm have the highest risk, and Cu with particle sizes of 0.5–1 mm has the highest pollution risk. The pollution risk assessment of Cr, Ni, and Cu based on the RSP method is higher than that based on the I_{geo} method, which was consistent with the research conclusion of Wei et al. [22]. This may be attributed to the fact that the soil accumulation index method primarily assesses the total amount of heavy metals in soil pollution, without taking into consideration the chemical reactivity and biological availability of heavy metals. In contrast, the RSP method also considers the correlation between the availability of soil heavy metals and the proportion of stable forms [29].

3.5. Differences in the Form Distribution of Heavy Metals in Aggregates of Different Particle Sizes

The RDA results are presented in Figure 6. The distributions of aggregates with particle sizes of 0.25–0.5 mm and 0.5–1.0 mm exhibit substantial overlap, suggesting similarity in the fundamental properties of these two aggregates. Specifically for Cr, the spatial distribution pattern of aggregates with a particle size range of 1–2 mm significantly deviates from that of other particle sizes, aligning closely with available phosphorus and SOM. This indicates that available phosphorus and SOM are the primary factors contributing to differences between this particular aggregate size and others. Available phosphorus and SOM exert positive influences on carbonate-bound of Cr, hydrolyzed nitrogen, CEC, and exchangeable calcium demonstrate positive effects on residual state of Cr; this is consistent with the finding that the proportion of Cr bound to carbonate and residual forms in aggregate particles is notably higher than in other particle sizes.

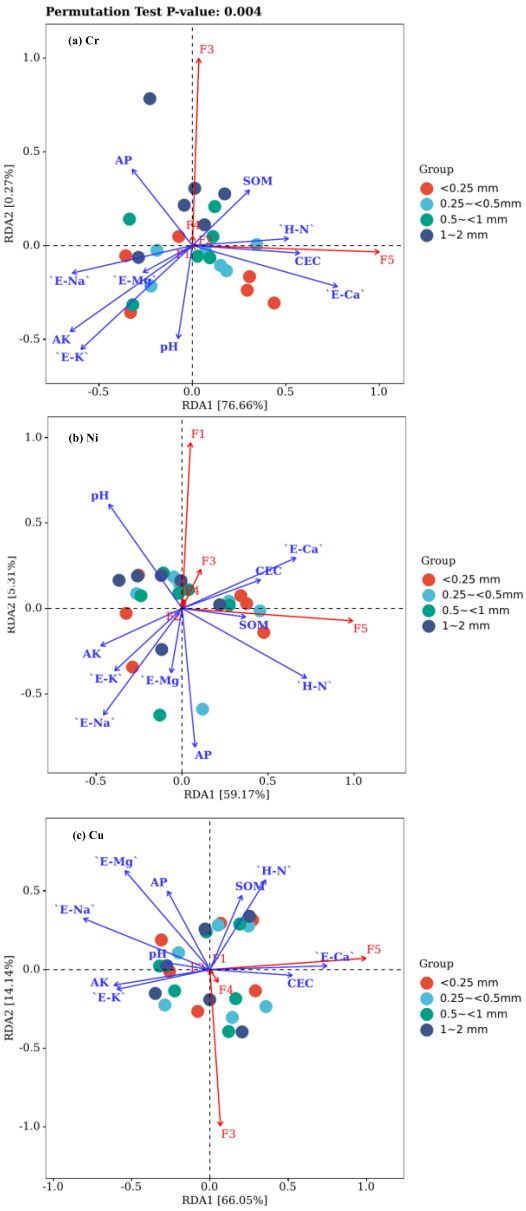

Figure 6. RDA analysis of heavy metal content and physicochemical properties in soil aggregates of different particle sizes. Note: Different colors of circles represent different particle sizes, and F1–F5 are Tessier five-step forms, respectively. The red line represents the value of Tessier's five-step form, and the blue line represents the values of various physical and chemical properties of soil.

For Ni, SOM, CEC, and exchangeable calcium positively impact both Fe-Mn-oxide binding of Ni as well as carbonate binding of Ni; thus indicating their significant roles in influencing morphological changes exhibited by Ni across different aggregate particle sizes [28]. Furthermore, the positive effects observed for heavy metals Cu along with CEC and exchangeable calcium on residual Cu suggest that CEC and exchangeable calcium play pivotal roles in shaping Cu morphology within various aggregate particle sizes [30].

3.6. Correlation Analysis of Total Amount and Available State Content for Heavy Metals and Physicochemical Properties

As shown in the Figure 7, it can be seen that there is a significantly positive correlation between heavy metals Cr, Ni, and Cu, and for Ni and Cu, there is also a significantly positive correlation between their respective total amount and the available content. This could be as a result of the strong homologous relationship between Cr, Ni, and Cu, hence, a rise in one of their concentrations may lead to compound pollution [31]. In addition, there is a significant positive correlation between SOM, hydrolyzable nitrogen, and CEC; available iron and available phosphorus. And there is also a significant positive correlation between CEC, exchangeable calcium, and exchangeable magnesium. This indicates that the cation exchange capacity of the soil in the study area is mainly determined by the contents of exchangeable calcium and exchangeable magnesium [32]. There is a significantly negative correlation between pH and available phosphorus, available iron. In addition, SOM, available potassium, CEC, exchangeable potassium, exchangeable magnesium, exchangeable calcium, and the contents of the three heavy metals were significantly negatively correlated. These findings suggest that exchangeable cations and SOM in soil have some influence on the concentration of heavy metals [33].

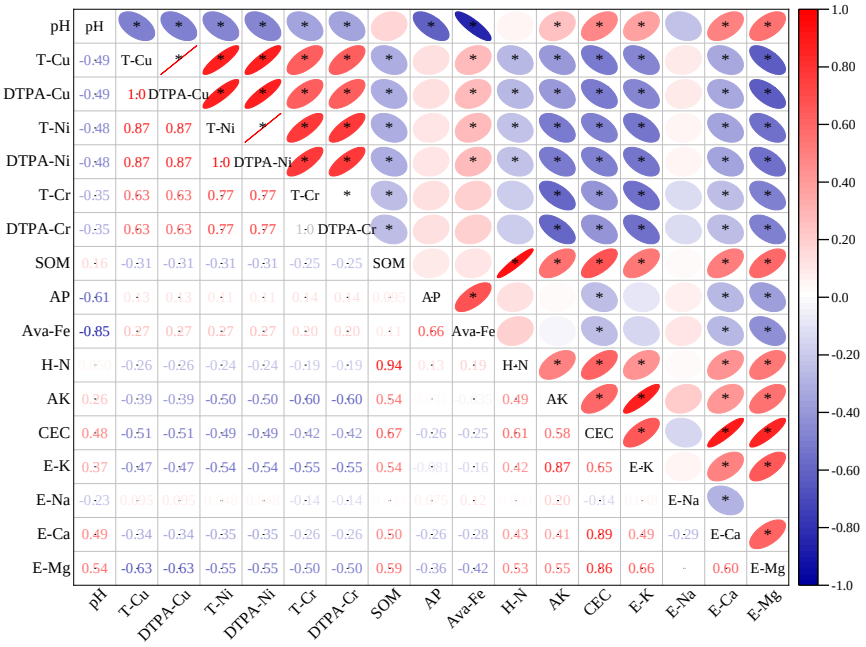

Figure 7. Correlation analysis of total amount and available state content for heavy metals and physicochemical properties. * The correlation is significant when the confidence level (both sides) is 0.05; a deeper color of red indicates stronger correlation, and a deeper color of blue indicates weaker correlation.

4. Conclusions

(1) In the horizontal direction, the contents of Cr, Ni, and Cu vary greatly, and their distribution is uneven. The pollution degree of Plot 4 is the least; in the vertical direction, there were Cr, Ni, and Cu pollution in deep soil samples of Plots 1, 2, 7, and 8. There is no increase or decrease relationship between heavy metal content and soil depth.

(2) In the particle size of soil aggregates, the distribution range of the particle size with the lowest content of heavy metals Cr, Ni, and Cu was <0.25 mm, the distribution range of the particle size with the highest content was 0.25–0.5 mm, and the heavy metal content decreased with the increase in the particle size range.

(3) The subsurface and surface forms of the polluted area are similar—Cr, Ni, and Cu mainly exist in the soil in residual states and Fe-Mn oxide combined states, and their forms are relatively stable. The morphology of the three heavy metals was not related to the size range of the aggregates.

(4) The I_{geo} evaluation showed that the pollution degree was Cr > Cu > Ni, and the Cr, Ni, and Cu in the soil layer aggregates of the three polluted plots were light pollution and moderate pollution, and none of them reached the severe pollution level. RSP results showed that Cr, Ni, and Cu were heavily polluted in soil of plot 1. RSP assessment of pollution risk is higher than ground accumulation index method.

(5) RDA and correlation analysis showed that available phosphorus, SOM, hydrolyzed nitrogen, CEC and exchangeable calcium were the main factors affecting the morphological changes of Cr. SOM, CEC and exchangeable calcium had a great influence on the morphological changes of Ni aggregates of different particle sizes, and CEC and exchangeable calcium were also the main factors affecting the morphological changes of Cu in the aggregates of different particle sizes.

Author Contributions: Writing—original draft, S.X.; investigation, J.Z.; formal Analysis, X.G.; conceptualization, Y.S.; writing—review and editing, Z.L. and Q.H. All authors have read and agreed to the published version of the manuscript.

Funding: This research was funded by Tianjin North China Geological Exploration Bureau, grant number HK2023-B14.

Data Availability Statement: The data that support the findings of this study are available from the corresponding author, upon reasonable request.

Acknowledgments: The author thanks the leaders and colleagues of 514 Brigade of North China Geological Exploration Bureau for their strong support to this study.

Conflicts of Interest: Authors Sha Xie, Jie Zhang, Zhijun Liu and Xiaofei Guo were employed by the company Hebei Huakan Resource Environmental Survey Co., Ltd. The remaining authors declare that the research was conducted in the absence of any commercial or financial relationships that could be construed as a potential conflict of interest.

References

1. Shi, J.; Zhao, D.; Ren, F.; Huang, L. Spatiotemporal variation of soil heavy metals in China: The pollution status and risk assessment. *Sci. Total Environ.* **2023**, *871*, 161768. [CrossRef]
2. Kumar, V.; Sharma, A.; Kaur, P.; Singh Sidhu, G.P.; Bali, A.S.; Bhardwaj, R. Pollution assessment of heavy metals in soils of India and ecological risk assessment: A state-of-the-art. *Chemosphere* **2019**, *216*, 449–462. [CrossRef]
3. Gautam, P.K.; Gautam, R.K.; Banerjee, S.; Chattopadhyaya, M.C.; Pandey, J.D. Heavy metals in the environment: Fate, transport, toxicity and remediation technologies. *Nova Sci. Publ.* **2016**, *60*, 101–130.
4. Tchounwou, P.B.; Yedjou, C.G.; Patlolla, A.K.; Sutton, D.J. *Heavy Metal Toxicity and the Environment*; Birkhäuser Verlag: Basel, Switzerland; Boston, MA, USA, 2012; pp. 133–164.
5. Briffa, J.; Sinagra, E.; Blundell, R. Heavy metal pollution in the environment and their toxicological effects on humans. *Heliyon* **2020**, *6*, e04691. [CrossRef]
6. Yuwono, S.B.; Banuwa, I.S.; Dermiyati, S.N.S.H. Mercury pollution in the soil and river water of the Ratai watershed by artisanal and small-scale gold mining activities in Pesawaran District, Lampung, Indonesia. *J. Degrad. Min. Lands Manag.* **2023**, *10*, 4233–4243. [CrossRef]
7. Gallego, L.; Fernández-Caliani, J.C. Pyrite ore cargo spills as a source of soil pollution and ecological risk along the abandoned railway corridors of the Tharsis and Rio Tinto mines (Spain). *Environ. Monit. Assess.* **2022**, *195*, 97. [CrossRef]
8. Hayyood, E.M.A.; Khalaf, A.A.; Obiad, M.M. Heavy metal maps of gypsiferous soil and its aassessment using geomatic and pollution indices in Baiji City. In Proceedings of the 5th International Conference of Modern Technologies in Agricultural Sciences, Montréal, QC, Canada, 17 April 2024.
9. Shen, Q.; Xiang, J.; Zhang, M. Distribution and chemical speciation of heavy metals in various size fractions of aggregates from zonal soils. *Int. J. Environ. Anal. Chem.* **2022**, *102*, 4272–4287. [CrossRef]

10. Deng, A.; Wang, L.; Chen, F.; Li, Z.; Liu, W.; Liu, Y. Soil aggregate-associated heavy metals subjected to different types of land use in subtropical China. *Glob. Ecol. Conserv.* **2018**, *16*, e00465. [CrossRef]
11. Zhang, F.; Cao, G.; Cao, S.; Zhang, Z.; Li, H.; Jiang, G. Characteristics and Potential Ecological Risks of Heavy Metal Content in the Soil of a Plateau Alpine Mining Area in the Qilian Mountains. *Land* **2023**, *12*, 1727. [CrossRef]
12. Qiang, Y.; Li, Y.J.; Luo, Q.; Chen, M.F.; Li, H.Y.; Huang, X.F. Relationship Characteristics and Risk Assessment of Heavy Metal Contents in Soil Aggregates and in Crops Around a Typical Pb-Zn Mining Area. *Environ. Sci.* **2021**, *42*, 5967–5976.
13. Cui, H.B.; Ma, K.; Fan, Y.; Peng, X.; Mao, J.; Zhou, D. Stability and heavy metal distribution of soil aggregates affected by application of apatite, lime, and charcoal. *Environ. Sci. Pollut. Res. Int.* **2016**, *23*, 10808–10817. [CrossRef]
14. Lu, R.K. *The Analysis Method of Soil Agricultural Chemistry*, 4th ed.; Chinese Agricultural Science Press: Beijing, China, 2000; pp. 12–295.
15. Bhutiani, R.; Kulkarni, D.B.; Khanna, D.R.; Gautam, A. Geochemical distribution and environmental risk assessment of heavy metals in groundwater of an industrial area and its surroundings, Haridwar, India. *Energy Ecol. Environ.* **2017**, *2*, 155–167. [CrossRef]
16. El-metwally, M.E.; Madkour, A.G.; Fouad, R.R.; Mohamedein, L.I.; Eldine, H.A.N.; Dar, M.A. Assessment the leachable heavy metals and ecological risk in the surface sediments inside the Red Sea ports of Egypt. *Int. J. Mar. Sci.* **2017**, *7*, 214–228. [CrossRef]
17. Sun, C.; Zhang, Z.; Cao, H.; Xu, M.; Xu, L. Concentrations, speciation, and ecological risk of heavy metals in the sediment of the Songhua River in an urban area with petrochemical industries. *Chemosphere* **2019**, *219*, 538–545. [CrossRef]
18. Wang, Y.J.; Li, L.L. Fractionation characteristics and ecological risk evaluation of metals in FCC spent catalysts. *Chem. Ind. Eng. Prog.* **2021**, *40*, 542–549.
19. Jiang, B.; Wang, S.T.; Sun, Z.B.; Zhang, H.R.; Wang, J.; Liu, Y. Evaluation of Cultivated Land Soil Fertility Based on Membership Function andPrincipal Component Analysis. *CASB* **2023**, *39*, 22–27.
20. Qian, Y.Y.; Ma, X.; Xia, J.J.; Wang, L.P.; Liu, X.R.T.; Zhang, Z.M.; Yan, H.; Li, Z.W.; Ni, M.; Wang, C. Spatial distribution characteristics and fertility quality evaluation of soil nutrients in tobacco-planting areas of the north central subtropical region of Yunnan province. *SCJAS* **2024**, *37*, 1–12.
21. Xi, X.H.; Hou, Q.Y.; Yang, Z.F.; Ye, J.Y.; Yu, T.; Xia, X.Q.; Cheng, H.X.; Zhou, G.H.; Yao, L. Big data based studies of the variation features of Chinese soil's backeround value reference value: A paper written on the occasion of Soil Geochemical Parameers of China's publication. *Geophys. Geochem. Explor.* **2021**, *45*, 1095–1108.
22. Wei, X.L.; Zhang, S.; Zhang, Y.L.; Ye, Z.H.; Chen, H.Y.; Li, Y.T.; Li, W.Y. Cd and Pb distribution characleristics and risk asesment in agricultural soil agregales surounding a zine smeller. *J. Agro-Environ. Sci.* **2023**, *42*, 820–832.
23. Singh, D.M.; Singh, S.; Ghoshal, N. *Soil Aggregates: Formation, Distribution and Management*; Nova Science Publishers, Inc.: New York, NY, USA, 2017; pp. 165–189.
24. Zhao, W.; Gu, C.; Ying, H.; Feng, X.; Zhu, M.; Wang, M. Fraction distribution of heavy metals and its relationship with iron in polluted farmland soils around distinct mining areas. *Appl. Geochem.* **2021**, *130*, 104969. [CrossRef]
25. Chen, X.C.; Wang, A.; Wang, J.J.; Zhang, Z.D.; Yu, J.Y.; Yan, Y.J. Influences of coexisting aged polystyrene microplastics on the ecological and health risks of cadmium in soils: A leachability and oral bioaccessibility based study. *J. Hazard. Mater.* **2024**, *469*, 133884. [CrossRef]
26. Qin, J.Q.; Zhao, H.R.; Dai, M.L.; Zhao, P.H.; Chen, X.; Liu, H.; Lu, B.Z. Speciation distribution and influencing factors of heavy metals in rhizosphere soil of miscanthus floridulus in the Tailing Reservoir area of Dabaoshan iron polymetallic mine in northern Guangdong. *Processes* **2022**, *10*, 1217. [CrossRef]
27. Wang, X.H.; Fan, F.; Zhang, L.H.; Qi, J.Y. Research progress on adsorption of heavy metals by manganese oxides and its influencing factors. *ACI* **2018**, *47*, 155–159.
28. Akbarpour, F.; Gitipour, S.; Baghdadi, M.; Mehrdadi, N. Correlation between chemical fractionation of heavy metals and their toxicity in the contaminated soils. *EES* **2021**, *80*, 1–12. [CrossRef]
29. Shi, Z.; Lu, J.; Liu, T.; Zhao, X.; Liu, Y.; Mi, J. Risk assessment and source apportionment of available atmospheric heavy metal in a typical sandy area reservoir in Inner Mongolia, China. *Sci. Total Environ.* **2024**, *912*, 168960. [CrossRef]
30. Liu, S.; Wu, K.; Yao, L.; Li, Y.; Chen, R.; Zhang, L. Characteristics and correlation analysis of heavy metal distribution in China's freshwater aquaculture pond sediments. *Sci. Total Environ.* **2024**, *931*, 172909. [CrossRef]
31. He, Y.; Wang, Z. Traceability Analysis of Heavy Metals in Soils Based on Data Analysis and Self-Organization Map Method. In Proceedings of the 2020 IEEE 11th International Conference on Software Engineering and Service Science (ICSESS), Beijing, China, 16 October 2020.
32. Chen, D.Y.; Wang, P.; Li, D.M.; Zhang, R.H.; Gao, B.Y.; Liu, S.Y. Correlation Analysis between pH and Organic Matter and Heavy Metal Content in Southern Agricultural Soil. *Adv. Anal. Chem.* **2023**, *13*, 410–417. [CrossRef]
33. Huang, X.; Li, N.; Wu, Q.; Long, J.; Luo, D.; Huang, X. Fractional distribution of thallium in paddy soil and its bioavailability to rice. *Ecotox Environ. Safe* **2018**, *148*, 311–317. [CrossRef]

Disclaimer/Publisher's Note: The statements, opinions and data contained in all publications are solely those of the individual author(s) and contributor(s) and not of MDPI and/or the editor(s). MDPI and/or the editor(s) disclaim responsibility for any injury to people or property resulting from any ideas, methods, instructions or products referred to in the content.